e-ISSN 2621-9883
Elipsoida: Jurnal Geodesi dan Geomatika
Vol 08, No 02, (2025)

LANDSLIDE VULNERABILITY ZONE MODELING BASED ON AHP-GIS AND GEOELECTRIC METHOD VERIFICATION: AN EARLY DETECTION STRATEGY IN SEBULU DISTRICT, KUTAI KARTANEGARA REGENCY

Rizky Fadillah[1], Djayus[2], Nanda Khoirunisa[1*]
[1]Program Studi Geofisika, Universitas Mulawarman, Jl. Barong Tongkok, Gn. Kelua, Kec. Samarinda Ulu, Kota Samarinda, Kalimantan Timur, INDONESIA – 75242
[2]Program Studi Fisika, Universitas Mulawarman, Jl. Barong Tongkok, Gn. Kelua, Kec. Samarinda Ulu, Kota Samarinda, Kalimantan Timur, INDONESIA - 75242
Corresponding author(s) e-mail: nandakhoirunisa@fmipa.unmul.ac.id

(Received 19 September 2025, Accepted 26 November 2025, Published 04 Desember 2025)

ABSTRACT

Landslides and soil movement frequently occur in Sebulu District, especially on the main access road. This study aims to analyze the vulnerability to landslides in Sebulu District, Kutai Kartanegara Regency, using the Analytical Hierarchy Process (AHP) and Geographic Information System (GIS) approaches, with verification through the geoelectric method. The advantage of this integrated approach is its ability to combine multi-criteria spatial modeling with physical validation of subsurface conditions, thereby producing a more comprehensive and reliable analysis. The secondary data used includes geological information, rainfall, slope gradient, soil type, and land cover. By applying AHP weighting, landslide vulnerability values were obtained with "low," "medium," and "high" categories, covering areas of 230.31 ha, 301.99 ha, and 309.30 ha, respectively. Verification using the geoelectric method identified a weak zone with a thickness of 1–5 meters, which could trigger soil movement towards the southwest. These results provide a clearer understanding of landslide-prone areas, which can serve as the basis for early detection strategies in disaster mitigation.

Keywords: susceptibility zones, landslide, geographic information system, AHP, geoelectric resistivity.

1. INTRODUCTION

Landslides occur when soil or rock on a slope moves downward, causing a terrestrial event involving ground movement. The main thrust on an inclined plane that exceeds the surface resistance of the sliding plane influences the occurrence of landslides. Factors such as rock strength, slope, water, load, and thickness of soil and rock influence the main driving force in landslides (Soehatman, 2010). People living on steep slopes are at risk of landslides (Wardyaningrum, 2014).

Landslides are caused by heavy rainfall, sudden changes in elevation, loose soil, soft rock, irregular land use, earth tremors, erosion, cliff embankments, discontinuity areas, deforestation, and improper waste disposal. One of the triggering factors for landslides in the research area due to slope failure is the slip plane, where soil/rock material will move above the plane and flow down the slope at high speed (Souisa, 2015). Rainwater seeps into the earth, causing the soil to become soft, damp and slippery. An increase in soil volume and weight of soil mass causes landslides. On a sliding surface, the soil will slip and, if the load is applied continuously, can result in a landslide (Naryanto, 2016).

Landslides are a dangerous geological phenomenon that often occur in areas with steep topography, especially along main roads, such as those in Sebulu District, Kutai Kartanegara. These landslides can be caused by various factors, such as high rainfall intensity, steep slopes, and soil instability (Soehatman, 2010; Naryanto, 2016). This phenomenon is highly detrimental, both socially and economically, and environmentally. Therefore, analyzing landslide vulnerability is crucial to provide a clear picture of the existing risks and to design appropriate mitigation measures.

Research related to landslides was conducted by Tunena (2018) in Tinor Village, North Tomohon, North Sulawesi, using geoelectric methods. The results revealed the structure of the subsurface layers and slip surfaces. Meanwhile, research by Hendra Lesmana (2016) in Samarinda Ilir, East Kalimantan, focused on identifying basement rock in landslide zones. This study revealed the location of slip surfaces, constituent rocks, and weak zones within the landslide area.

Meanwhile, research by Fauzi et al. (2019) demonstrated that the use of geoelectric methods can detect areas with low resistivity that have the

potential to act as weak zones in landslide systems. This was demonstrated by the application of geoelectric techniques to identify slip surfaces in hilly areas. This combination of GIS and geoelectricity provides a more holistic approach to identifying potential vulnerabilities, making it more effective in designing appropriate mitigation measures.

Although research on landslide vulnerability has been carried out extensively previously (Bayuaji et al., 2016; Wibowo et al., 2018), However, most of them use conventional methods that are less effective in handling the complexity of spatial data. This study integrates the AHP-GIS and geoelectric approaches, where AHP-GIS is used for multi-criteria spatial modeling in mapping vulnerability zones, while geoelectricity serves as a physical verification method to confirm subsurface conditions (such as slip planes) in risk areas. By considering geological factors, rainfall, and topographic conditions comprehensively, this study is expected to provide important contributions in vulnerability mapping and disaster mitigation strategies.

2. RESEARCH METHODS

This study uses a quantitative approach that combines spatial analysis (AHP-GIS) and geophysical surveys (geoelectric). The research location is in Sebulu District, Kutai Kartanegara Regency, which is geographically located at coordinates 117°2'3"E and 0°11'47.1"S. The regional stratigraphic setting of the study location is composed of volcanic rocks, shale, sandstone intercalations, coal, and quartz (Supriyatna, 1995).
The geoelectric resistivity survey aims to identify subsurface structures, particularly layers that have the potential to become slip surfaces. Data collection was conducted at the Giri Agung Village road axis, which was selected based on historical reports of landslides and initial observations indicating cracks in the road surface. Three measurement paths were established in the identified most at-risk areas to map lateral and vertical variations in subsurface conditions. The resistivity values measured in the field were calculated using the formula:

$$K = 2\pi a \quad (1)$$

$$K\left(\frac{V}{I}\right)\rho a = \Delta v \quad (2)$$

The equation depends on the electrode spacing (Sapulete, 2012), where ρa is the apparent resistivity (Ω.m), ΔV is the potential difference (volt), I is the current strength (A) and K is the geometry factor (m) for the Wenner–alpha configuration (Telford, 2004), a (m) is the distance between the two current electrodes equal to the distance between the two potential electrodes and n= 1,2,3,4,... The field data obtained are then processed through an inversion process to produce a 2D resistivity cross-section model that describes the actual subsurface conditions (Souisa, 2015).

Landslide vulnerability zone mapping is conducted to determine reference points, including sampling to obtain data on factors influencing landslide occurrence. Parameters used for field observations include rainfall, slope, geological structure, land use, soil type, earthquakes, and faults. These parameters are then weighted according to their influence on landslide occurrence, as determined by the Ministry of Public Works (Pattiselanno, 2014). Landslide hazard assessment for natural physical aspects was conducted by summing the weighted values of seven indicators. Then, a quantitative spatial analysis method was used, utilizing Geographic Information System (GIS) technology, using a landslide hazard zoning model (Paimin, 2009). After new spatial data is generated, data classification is carried out based on certain criteria for the data studied by providing a score value divided into three zones of vulnerability levels to landslide hazards in landslide hazard areas (Sarkar, 2004). The landslide hazard distribution map is used as a reference for mapping landslide hazard risks.
Thomas L. Saaty created the Analytical Hierarchy Process (AHP) approach as a decision-making tool. Using this model, complex multi-criteria problems are resolved into a hierarchical structure, where the hierarchy serves as a multi-level representation of the difficult problem. Complex problems can be divided into groups using the hierarchy, and these groups can then be organized hierarchically to give the impression of greater order and systematicity (Syaifullah, 2010).

The methods used in this study consist of two main approaches: AHP-GIS and geoelectric resistivity. Data collection was carried out through field observations and secondary data collection from geological maps, rainfall maps, slope maps, as well as soil type and land cover data. The obtained data were then analyzed using AHP to determine the weight and score of each parameter, such as slope gradient, rainfall, soil type, and land use (Saaty, 1980; Syaifullah, 2010).

To verify landslide-prone soil layers, geoelectric measurements were conducted using the Wenner-Alpha configuration on several tracks in areas

identified as prone to landslides. Geoelectric data processing produced 2D cross-sections depicting the resistivity of the soil and subsurface layers. This resistivity data was then analyzed to identify weak zones and slip surfaces, which could lead to landslides, in accordance with geoelectric theory (Telford et al., 2004).

The AHP method uses a pairwise comparison matrix to convert qualitative ratio data and access criteria weights using eigenvalues and consistency indices (Vahidnia et al., 2009). The data used in the analysis are: a) Secondary Geoelectric Resistivity Data of Wenner–Alpha configuration; b) Regional Geological Map; c) Land Cover Map; d) Rainfall Map; e) Soil Permeability Map; f) Slope Map. Each parameter related to landslides is given a score, which is then multiplied by the weight of each parameter that influences the possibility of landslides (Taufiq, 2008). The following is a classification of parameters used in this study:

Table 1. Parameter Classification, Weight (%), and Score

Classification	Value	Weight (%)	Score
Land Slope (Matondang, J.P., 2013)			
Flat (0%≤Ø≤8%)	1	30	0,3
Sloping (8%<Ø≤15%)	2	30	0,6
A bit steep (15<Ø≤25)	3	30	0,9
Steep (25<Ø≤45)	4	30	1,2
Very Steep 45<Ø	5	30	1,5
Soil Permeability (Taufiq, 2008)			
Very bad	1	10	0.1
Bad	2	10	0.2
Medium	3	10	0.3
Good	4	10	0.4
Geological Formation (Sarkar & Kanungo, 2004)			
Kampungbaru Formation	8	10	0.8
Shallow Sandstone	1	10	0.1
Balikpapan Formation	6	10	0.6
Pulaubalang Formation	5	10	0.5
Babulu Formation	1	10	0.1
Pamalun Formation	4	10	0.4
Land Cover (Taufiq, 2008)			
Open Land	1	20	0.2
Forest/plantation	2	20	0.4
Settlement	3	10	0.6
Rice fields	4	10	0.8
Annual Rainfall (mm/month) (Permen PU No. 22, 2007)			
2.848,9-2.855,2	1	20	0.8
2.855,2-2.861,6	2	20	0.6
2.861,6-2.867,9	3	20	0.4
2.867,9-2.874,3	4	20	0.2

Table 2. Parameter matrix values (Taufiq, 2008)

Matrix Value	Parameter
3	Slope Gradient
2	Annual Rainfall
2	Land Cover
1	Regional Geology
1	Soil Permeability

The weight value and normalization of parameter values are determined by comparing the intensity of each parameter and then normalizing the comparison results by calculating the total and dividing by the total number of values (Taufiq, 2008). The following is the weighting procedure for analyzing landslide vulnerability based on AHP-GIS:

Table 3. Parameter Weighting Procedure

	Comparison				
Parameter	**Slope Gradient**	**Annual Rainfall**	**Land Cover**	**Geology**	**Soil Permeability**
Slope Gradient	1	$\frac{3}{2}$	$\frac{3}{2}$	3	3
Annual Rainfall	$\frac{2}{3}$	1	1	2	2
Land Cover	$\frac{2}{3}$	1	1	2	2
Regional Geology	$\frac{1}{3}$	$\frac{1}{2}$	$\frac{1}{2}$	1	1
Soil Permeability	$\frac{1}{3}$	$\frac{1}{2}$	$\frac{1}{2}$	1	1
Total Weight	3	4,5	4,5	9	9

Table 4. Parameter Normalization Procedure

	Normalization				
Parameter	**Slope Gradient**	**Annual Rainfall**	**Land Cover**	**Geology**	**Soil Permeability**
Slope Gradient	0,33	0,33	0,33	0,33	0,33
Annual Rainfall	0,22	0,22	0,22	0,22	0,22
Land Cover	0,22	0,22	0,22	0,22	0,22
Geology	0,11	0,11	0,11	0,11	0,11
Soil Permeability	0,11	0,11	0,11	0,11	0,11

Total	0.99	0,99	0,99	0,99	0,99

Table 5. Parameter Weight Table

Parameter	Weight
Slope Gradient	0,33
Annual Rainfall	0,22
Land Cover	0,22
Geology	0,11
Soil Permeability	0,11

The first step in determining the consistency index is to multiply the weights of each parameter to determine its weight value. The ratio of the parameter value to the corresponding weight is then used to calculate the parameter value, as shown in **Table 6**.

Table 6. Weighted Parameter Sum and Parameter Consistency

Parameter	Total Parameter Weighting	Index Consiste-ncy
Slope Gradient	$(0{,}33\ x\ 1) + \left(0{,}22\ x \frac{3}{2}\right) + \left(0{,}22\ x \frac{3}{2}\right) + (0{,}11\ x\ 3) + (0{,}11\ x\ 3) = 1{,}65$	$\frac{1.65}{0.33} = 5$
Annual Rainfall	$\left(0{,}33\ x \frac{2}{3}\right) + (0{,}22\ x1) + (0{,}22\ x1) + (0{,}11\ x\ 2) + (0{,}11\ x\ 2) = 1{,}1$	5
Land Cover	$\left(0{,}33\ x \frac{2}{3}\right) + (0{,}22\ x1) + (0{,}22\ x1) + (0{,}11\ x\ 2) + (0{,}11\ x\ 2) = 1{,}1$	5
Geology	$\left(0{,}33\ x \frac{1}{3}\right) + \left(0{,}22\ x \frac{1}{2}\right) + \left(0{,}22\ x \frac{1}{2}\right) + (0{,}11\ x\ 1) + (0{,}11\ x\ 1) = 0{,}55$	5
Soil Permeability	$\left(0{,}33\ x \frac{1}{3}\right) + \left(0{,}22\ x \frac{1}{2}\right) + \left(0{,}22\ x \frac{1}{2}\right) + (0{,}11\ x\ 1) + (0{,}11\ x\ 1) = 0{,}55$	5

3. RESULTS AND DISCUSSION

3.1. Landslide Hazard Index

The geological map of the research area was obtained from the geological map sheet of Samarinda (Supriatna et al. 1995). In **Figure 1** the area bounded by the red line is the Sebulu District area which has an area of 59,969.72 Ha. This area is included in the arrangement of four rock formations namely the Pamaluan Formation (Tomp), the Balang Island Formation (Tmpb), and Alluvial Deposits (Qa), and the Balikpapan Formation (Tmbp). While at the Geoelectric measurement point it is included in the Pamaluan Formation (Tomp). The four types of Geological Formations above have an area in hectares including, the Pamaluan Formation has an area of 30,646.06 Ha with a percentage of 32.23% spread across Mekar Jaya Village, Manunggal Daya Village, Sumber Sari Village, Sebulu Modern Village, Beloro Village, Tanjung Harapan Village, Senoni Village, Sanggulan Village, Giri Agung Village, and Segihan Village; The Balang Island Formation has an area of 19,733.96 Ha with a percentage of 20.75% spread across Sumber Sari Village, Sebulu Modern Village, Beloro Village, Tanjung Harapan Village, Sanggulan Village, Sebulu Ulu Village; Sebulu Ilir Village, and Giri Agung Village; Alluvial Deposits have an area of 5,382.76 Ha with a percentage of 5.66% spread across Mekar Jaya Village; Manunggal Daya Village, and Lekaq Kidau Village; and Balikpapan Formation Deposits have an area of 3,130.45 Ha with a percentage of 3.29% spread across Mekar Jaya Village; Manunggal Daya Village, and Lekaq Kidau Village.

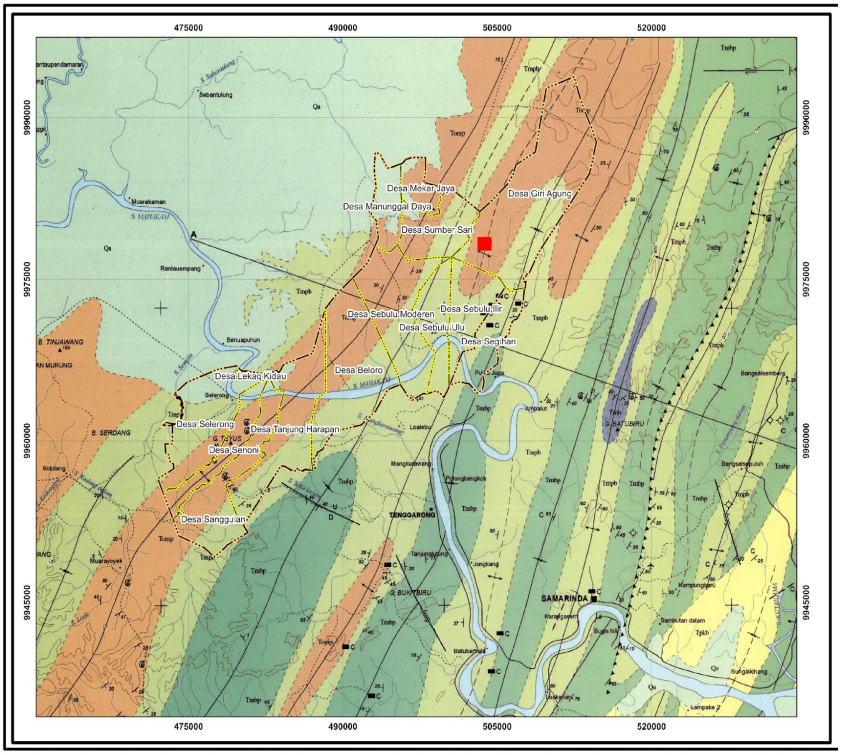

Figure 1. Regional Geological Map of Sebulu District

Based on the data obtained from the attribute table (**Figure 2**), Sebulu District, Kutai Kartanegara Regency has 4 categories of rainfall classes, namely the first class 2600-2700 mm/year; 2700-2800 mm/year; 2800-2900 mm/year; and 2900-3000 mm/year in a period of 1 year with the number of rainy months being 52 weeks in 2022.

The four classifications of rainfall intensity above have an area in hectares, including, in the range of 2600-2700 mm/year has an area of 1,108.68 Ha with a percentage of 1.82% which is spread only in Lekaq Kidau Village; in the range of 2700-2800 mm/year has an area of 1,185.94 Ha with a percentage of 19.46% which is spread in several villages including Lekaq Kidau Village, Senoni Village, Selerong Village, Tanjung Harapan Village, Segihan Village and Mekar Jaya Village; in the range of 2800-2900 mm/year has an area of 26,585.29 Ha with a percentage of 43.53% which is spread in several villages including Sanggulan Village, Segihan Village, Tanjung Harapan Village, Beloro Village, Sebulu Modern Village, Sebulu Ulu Village, Sebulu Ilir Village, Sumber Sari Village, Manunggal Daya Village, Mekar Jaya Village, and Giri Agung Village; and in the range of 2900-3000 mm/year has an area of 21,498.87 Ha with a percentage of 35.2% spread across several villages including Beloro Village, Sanggulan Village, Sebulu Modern Village, Sebulu Ulu Village, Sebulu Ilir Village, and Giri Agung Village.

Figure 3 shows that the slope of Sebulu District ranges from 0 to 163°. Slope gradient can cause soil or rock masses to move from higher to lower elevations, significantly impacting landslides. Among other parameters, slope gradient has the highest intensity because landslides frequently occur on relatively steep slopes, which play a significant role in landslide occurrence.

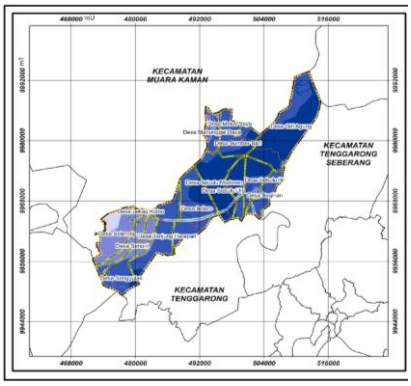

Gambar 2. Rainfall map of Sebulu District

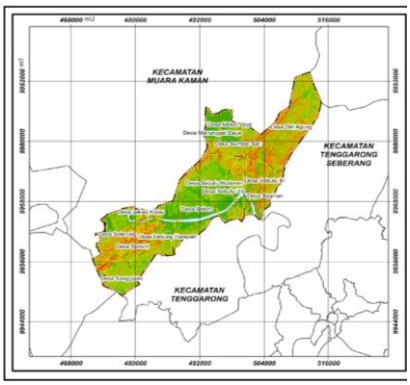

Gambar 3. Slope Map of Sebulu District

The four slope classifications above have areas in hectares: 6,750.34 ha for a slope range of 0°-8°; 5,781.78 ha for a slope range of 9°-18°; 5,557.11 ha for a slope range of 18°-29°; and 29°-163°; 29,525.66 ha. The higher the slope and the higher the percentage, the steeper the slope. Steep slopes and high rainfall intensity are key factors contributing to landslides.

Figure 4 shows that the soil types in Sebulu District are clay loam, loam, and sandy loam. The three soil types mentioned above are measured in hectares. Clay loam covers 23,064.69 ha, representing 38.46% of the total area, spread across several villages, including Sanggulan, Sumber Sari, Manunggal Daya, Mekar Jaya, and Giri Agung. Loam covers 14,783.44 ha, representing 24.65% of the total area, spread across several villages, including Lekaq Kidau, Beloro, Sebulu Modern, Sebulu Ulu, Sebulu Ilir, and Segihan. Sandy loam covers 22,121.97 ha, representing 36.89% of the total area, spread across several villages, including Sanggulan, Senoni, Selerong, Tanjung Harapan, Manunggal Daya, and Mekar Jaya.

Sebulu District has clay loam soil. The characteristics of clay loam are: Its texture is fine. When dry, this soil will break into hard lumps. When wet, this soil will form thin, tough rods that are difficult to break. The finer the soil texture, the more water it can store and its permeability is slow.

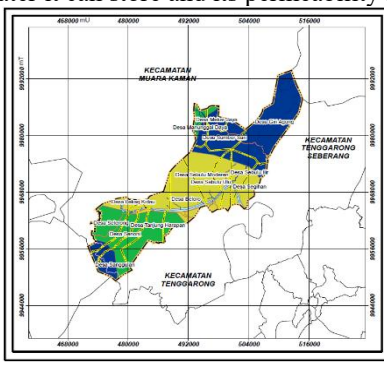

Figure 4. Sebulu District Soil Type Map

Figure 5 shows that the land use of Sebulu District is dominated by forests covering 46,837.95 ha with a percentage of 78.20%. The rest is open land covering 25.58 ha with a percentage of 0.04%. Residential areas covering 1,381.08 ha with a percentage of 2.31%. Plantations covering 3,917.94 ha with a percentage of 6.54%. Rice fields covering 451.90 ha with a percentage of 0.75%. And shrubs covering 5,274.67 ha with a percentage of 8.81%. Each of these variables was then classified to obtain land cover parameters in the study area. Sebulu District is also dominated by forests and a little shrubs.

The vulnerability map of the Sebulu District area resulting from the AHP analysis shows three vulnerability zones: low, medium, and high, with the high zone area identified in areas with steep slopes and soil that is easily saturated with water based on Figure 6. This is in line with the findings found by Lesmana (2016), which shows that areas with slopes of more than 30 degrees and high rainfall intensity have greater potential vulnerability.

Table 7. Landslide Vulnerability Classification of Sebulu District

Vulnerability	Color Symbols	Area	Precentage (%)
Low	Green	121.8 Ha	20.75%
Medium	Yellow	337.70 Ha	57.53%
High	Orange	127.31 Ha	21.69%
Very High	Red	0.20 Ha	0.03%

The application of the AHP method in disaster vulnerability analysis has made a significant contribution to the development of mitigation policies and risk-responsive spatial planning. Through a weighted-criteria approach based on factors such as slope gradient, land use, rainfall, soil type, and population density, this method produces a systematic and measurable vulnerability zoning classification. One practical implication of this study is the creation of a vulnerability map that can serve as a basis for determining disaster management priorities by local governments. Research conducted by Wibowo et al. (2018) demonstrated that the use of the AHP method was able to identify high-risk zones for landslides in the Banjarnegara region, which was then utilized in the development of contingency plans by relevant institutions.

In terms of policy impact, the results of AHP-based vulnerability assessments influence decision-

making in determining priority locations for structural and non-structural interventions. Areas with high levels of vulnerability can be targeted as primary development projects for disaster mitigation infrastructure, such as early warning systems, landslide-retaining structures, and community empowerment programs. As Herlina and Suharyanto (2020) noted, the integration of the AHP and Geographic Information Systems (GIS) methods in flood studies in the Bengawan Solo watershed successfully produced accurate vulnerability maps, which were subsequently used as a basis for risk reduction efforts by various stakeholders.

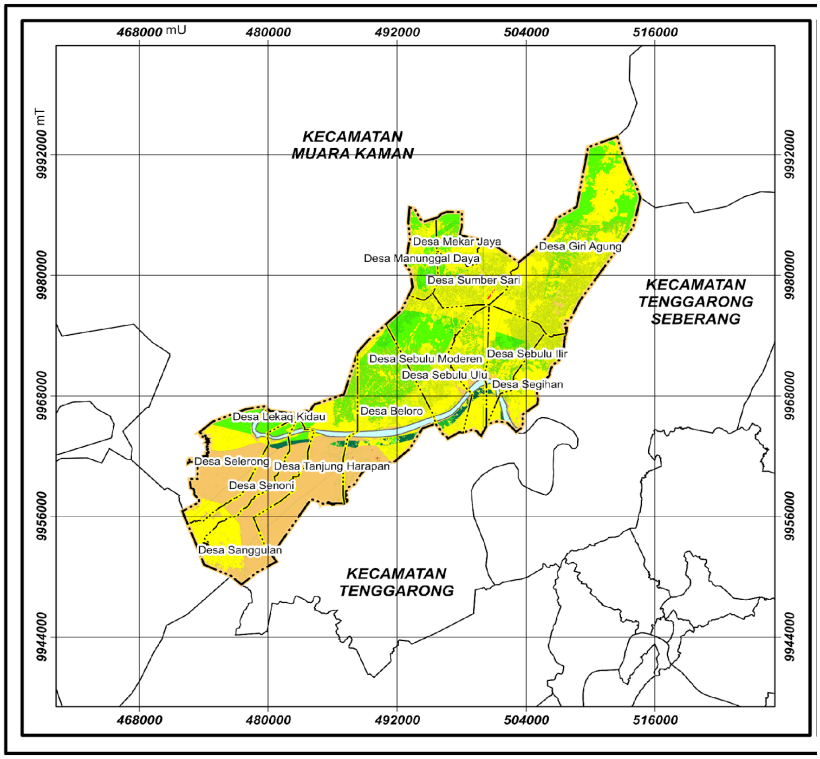

Figure 6. Landslide Vulnerability Map of Sebulu District

3.2 Geoelectric Resistivity Method Analysis

a) Track 1

Based on the results of data processing with data processing software in the form of a 2D cross-section with a path length of 141 meters and a spacing between electrodes of 3 meters. The starting point of the measurement is located at coordinates 0°11`46.64" South Latitude and 117°2`4.49" East Longitude while the end point of the measurement is located at coordinates 0°11`46.51" South Latitude and 117°2`0.41" East Longitude. In the 2D resistivity cross-section on path 1 using 4 iterations and obtained an RMS error of 16.5% as seen in **Figure 7.**

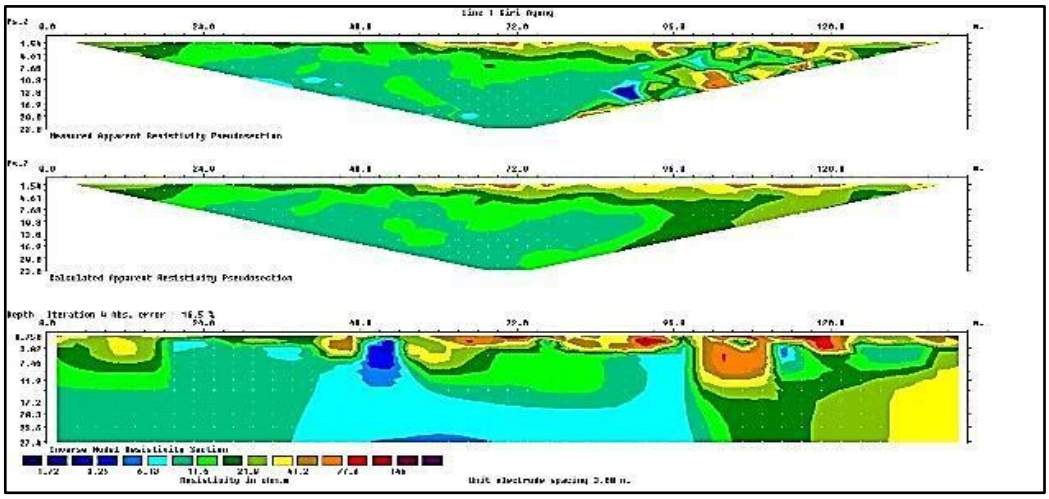

Figure 7. 2D Geoelectric Cross-Section Results of Track 1

Figure 7 a) is a cross-section of the measured values and does not yet represent the original resistivity value, b) is the result of the resistivity value calculation added with a geometric factor. This process still needs to be inverted to obtain the actual resistivity produced in the image; b). In Figure 7. c) this is the error value determined. The inversion model shows that on track 1, rocks consisting of wet soil with resistivity values ranging from 1.70 – 5.41 with units of Ωm at a depth of ±1 – 27.3 meters are identified as low resistivity and identified as a weak zone. This lithology is symbolized by light blue and dark blue colors that spread over a track distance of 40-98 meters. This estimate is based on Telford et al. (1990) yang menyatakan tanah yang bersifat basah which states that wet or watery soil has a resistivity range of 0.5 Ωm – 105 Ωm. The second layer is a clay layer with resistivity values ranging from 9.65 to 30.7 Ωm at a depth of ±1 to 27.3 meters. This lithology is symbolized by light green, dark green, and yellow colors, which are distributed over almost the entire distance of the track.

b) Track 2

The starting point of the measurement is located at coordinates 0°11`46.12" South Latitude and 117°2`4.20" East Longitude while the end point of the measurement is located at coordinates 0°11`46.51" South Latitude and 117°2`0.06" East Longitude. In the 2D resistivity cross-section on path 2, 4 iterations were used and an RMS error of 24.6% was obtained as shown in **Figure 8**.

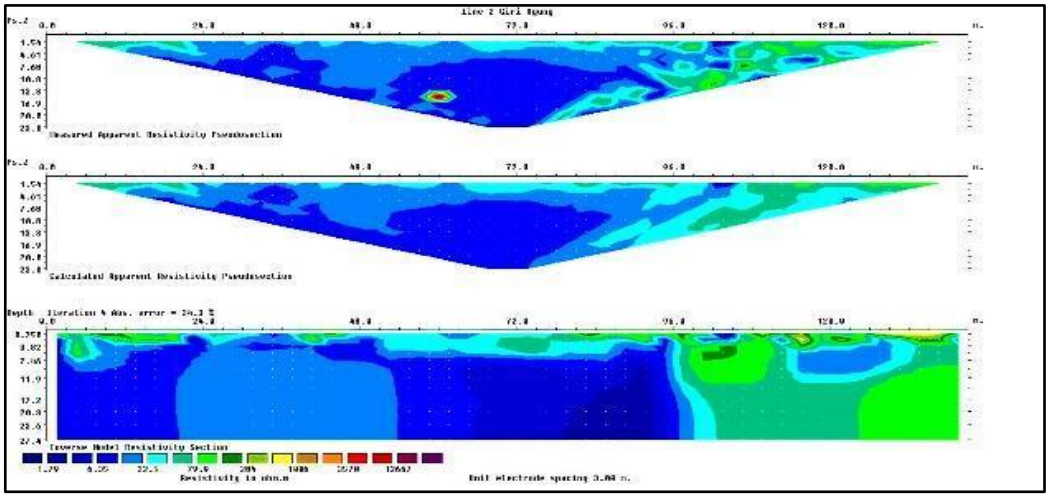

Figure 8. 2D Geoelectric Cross-Section Results of Track 2

Based on the data processing results on track 2, it can be identified that the rocks are composed of wet soil with resistivity values ranging from 1.70 – 22.00 Ωm at a depth of ±1 – 27.3 meters, which has a low resistivity value and is identified as a weak zone. This lithology is symbolized by light blue and dark blue colors that spread over a track distance of 0-100 meters. The lowest resistivity

symbolized by dark blue is very often found on this track. The second layer is a layer of claystone with resistivity values ranging from 78.2 – 993 Ωm, there is also a layer of claystone with sandstone inserts with resistivity values ranging from 3537 – 10000 Ωm at a depth of ±1 – 27.3 meters. Clay lithology is symbolized by dark green and light green and dominates the track distance of 100-141 meters.

c) Track 3

The starting point of the measurement is located at coordinates 0°11`46.84" South Latitude and 117°2`4.557" East Longitude while the end point of the measurement is located at coordinates 0°11`46.51" South Latitude and 117°2`0.125" East Longitude. In the 2D resistivity cross-section on path 3, 4 iterations were used and an RMS error of 34.9% was obtained as shown in **Figure 9**.

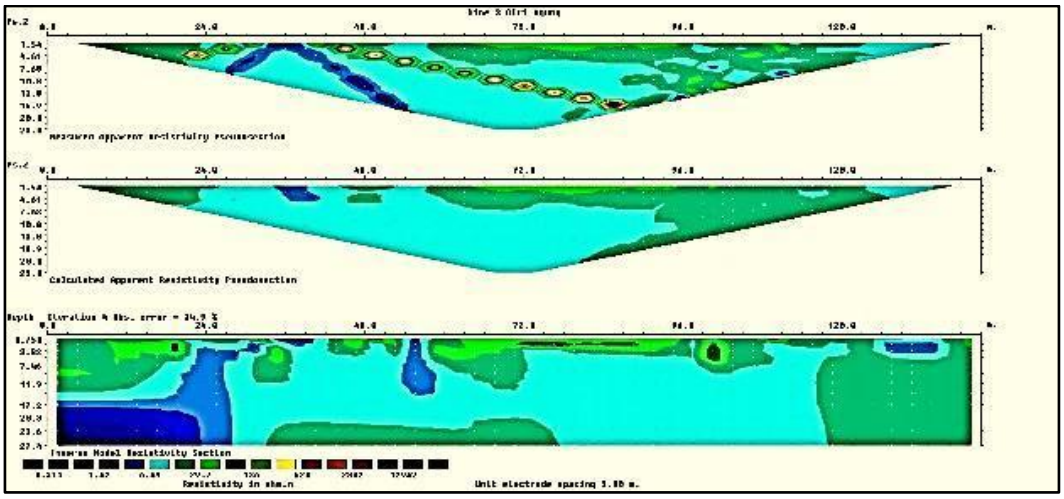

Figure 9. 2D Geoelectric Cross-Section Results of Track 3

Based on the data processing results on track 3, rocks composed of wet soil with resistivity values ranging from 0.311 to 6.49 Ωm at a depth of ±1 to 27.3 meters can be identified, which has low resistivity and is identified as a weak zone. This lithology is symbolized by light and dark blue colors spread over a track distance of 0-140 meters. The lowest resistivity is symbolized by dark and light green.

a.

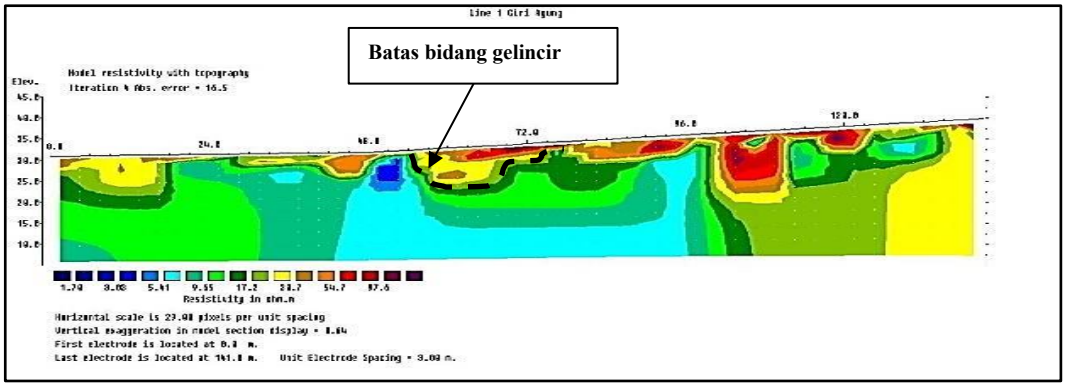

b.

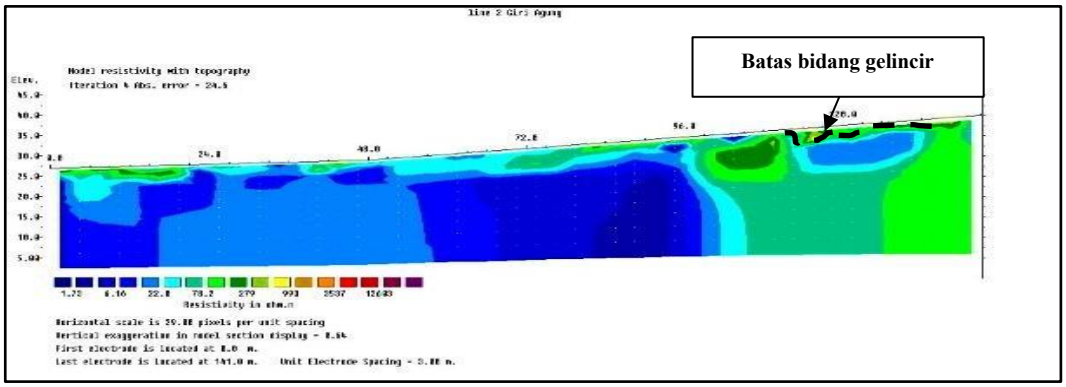

c.

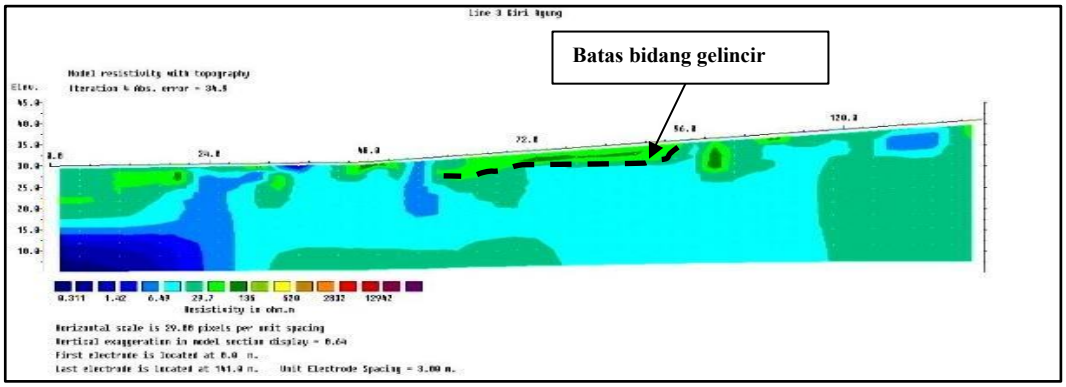

Figure 10. 2D cross-section of the track with topography, a) track I; b) track 2; c) track

The study area was identified as having a lithology consisting of wet soil (soil with high water saturation) and claystone. This is evidenced by resistivity values associated with the Telford (1990) rock resistivity table, the original conditions of the study area, and the rock formations on the geological map. The topography is sloping. The wet soil material (soil with high water saturation) is excellent at absorbing water, making this layer highly saturated.

The uppermost layer, which contains a large amount of water, is highly susceptible to landslides. Claystone is interpreted as a slip plane because it is recognized as a weak zone whose slope adapts to the topography. During heavy rainfall, some rainwater collects in this weak zone, the area between the slip plane boundary and the overlying soil layer. The slip plane on each trajectory is indicated by a dashed black line, with the dark blue line at a depth of 27 meters at a trajectory distance of 1-24 meters. The second layer is a layer of claystone with a resistivity value ranging between 29.7 – 620 Ωm, and there is also a layer of claystone with sandstone inserts with a resistivity value ranging between 2832 – 10000 Ωm at a depth of ±1 – 27.3 meters, symbolized by the color orange and spread throughout the track.

This slip indicates the potential for ground movement or landslides in the area. In the context of engineering or disaster mitigation planning, understanding the location and depth of slip plane boundaries is essential for assessing risk and planning effective prevention efforts.

The implications of the results in Figure 10, related to soil or slope stability analysis, are that these slip boundary lines indicate the potential for ground movement or landslides in the area. In the context of engineering planning or disaster mitigation, understanding the location and depth of slip boundary planes is crucial for assessing risk and planning effective prevention efforts.

In addition to the slip plane factor, several other parameters also influence landslide occurrence. These parameters are measured using a geographic information system method using an overlay technique. The parameters in question are geological conditions, rainfall intensity, land use, soil type, and slope gradient. The overlay technique uses Analytical Hierarchy Process weighting with weighted values. Each parameter class is assigned an appropriate weight and rank as attribute information in the Information System. Geoelectric test results provide important insights into subsurface conditions, particularly in identifying rock layers, weak zones, slip planes, and fractures that have the potential to become water passageways. If the resistivity results show a low

value (<100 Ωm), this can indicate the presence of loose material such as water-saturated clay or weak zones, which have a significant impact on slope stability. Conversely, high resistivity (>1000 Ωm) generally indicates dense or dry rock layers. Therefore, resistivity values directly influence the interpretation of landslide potential, groundwater saturation, and aquifer zones. The effect of the presence of low resistivity zones, for example, is increased vulnerability to landslides because these zones often act as slip surfaces due to water saturation. Causally, high rainfall causes an increase in groundwater, which then affects the decline in resistivity values in certain layers, and ultimately can trigger slope failure. In a study by Fauzi, et al., (2019), the use of resistivity methods was able to detect slip surfaces associated with landslides in hilly areas. Similarly, based on research (Soisa, 2015), to minimize subsequent landslides, a water highway model is used by utilizing small/large rivers located below the slope/cliff to channel water during the rainy season. The water highway model is integrated with geoforestry and bioengineering technology approaches so that landslide problems can be optimally reduced.

4. CONCLUSIONS AND SUGGESTIONS

Based on the research results, it can be concluded that AHP-GIS modeling classifies Sebulu District as having a moderate to high level of landslide vulnerability, reaching >79% of the total area. The dominant contributing factor is the geological conditions, with lithology that is easily saturated with water, even though rainfall in the area is not classified as extreme.

In this study, the geoelectric resistivity method served as a verification tool to confirm the results of the AHP-GIS spatial modeling. The geoelectric survey successfully identified weak zones with low resistivity values (0.311–22.00 Ωm), which are interpreted as water-saturated layers and have the potential to become slip surfaces. Meanwhile, claystone has a higher resistivity (9.65–993 Ωm), but can still contribute to landslides, especially if there are intercalations of sandstone with very high resistivity (2,832–10,000 Ωm). There is a strong and consistent correlation between the high-susceptibility zones mapped by AHP-GIS and the locations of weak zones detected through geoelectrical analysis. This combination demonstrates the effectiveness of AHP-GIS for large-scale mapping, while geoelectrical methods provide crucial physical validation of subsurface conditions.

For further development, it is recommended to develop an early warning system (EWS) by integrating these vulnerability maps with real-time rainfall monitoring. Further research could also involve in-depth geotechnical analysis at high-risk locations to quantify slope stability parameters, as well as applying complementary geophysical methods to improve the accuracy of slip plane identification..

REFERENCES

Bayu Aji, et al., (2016). *Analisis Penentuan Zonasi Risiko Bencana Tanah Longsor Berbasis Sistem Informasi Geografis (Studi kasus : Kabupaten Banjarnegara)*. *Jurnal Geodesi Undip*, Volume 5, Nomor 1, Tahun 2016, 326-335.

Fauzi, A., Sukobar, S., Wahyudi, D. I., & Moeljono, R. A. T. (2019). *Analisa stabilitas lereng dan alternatif penanganannya: Studi kasus proyek pekerjaan kanal utama Row 80 kawasan industri JIIPE-Gresik*. *Jurnal Aplikasi Teknik Sipil*, 17(2), 59–66. http://iptek.its.ac.id/index.php/jats/article/view/6228

Herlina, N., & Suharyanto, S. (2020). *Analisis kerentanan banjir berbasis AHP dan SIG di DAS Bengawan Solo. Jurnal Teknik ITS*, 9(2), A90–A95. https://doi.org/10.12962/j23373539.v9i2.56167

Lesmana, H. (2016). *Identifikasi Basement Rock pada Zona Longsor Dengan Menggunakan Metode Geolistrik (Studi Kasus Wilayah Kelurahan Selili Kecamatan Samarinda Ilir Kota Samarinda Kalimantan Timur)*. Prosiding Seminar Sains dan Teknologi FMIPA Unmul, 32-36.

Matondang, J. P., Kahar, S., & Sasmito, B. (2013). *Analisis zonasi daerah rentan banjir dengan pemanfaatan sistem informasi geografis (Studi kasus: Kota Kendal dan Sekitarnya*). *Jurnal Geodesi Undip*, 2(2).

Naryanto, Sri Heru. (2016). *Analisis Kejadian Bencana Tanah Longsor Tanggal 12 Desember 2014 Di Dusun Jemblung, Desa Sampang, kecamatan Karangkobar, Kabupaten Banjarnegara, Provinsi Jawa Tengah*. *Jurnal Alami*, Vol. 1 No. 1.

Paimin, et al. (2009). T*eknik Mitigasi Banjir dan Tanah Longsor*. Balikpapan: Tropenbos International Indonesia Programme.

Pattiselanno, S.R.R., Anwar, M.R. & Hasyim, A.W. (2014). *Handling Landslide Region*

watershed of Wai Ruhu. J*urnal Rekayasa Sipil*, 8 (1), 17–29.

Permen PU No. 22. (2007). *Peraturan Menteri Dalam Negeri Nomor 12 Tahun 2007 tentang Pedoman Penyusunan dan Pendayagunaan Data Profil Desa dan Kelurahan.* Direktorat Jenderal Pemberdayaan Masyarakat dan Desa (Ditjen PMD) Kementerian Dalam Negeri RI: Jakarta.

Sapulete, M.S., Sismanto, & Souisa, M. (2012). *Mapping of Lateritic Nickel Deposit Using Resistivity Method at Gunung Tinggi Talaga Piru, Western Seram Regency, Mollucas Province*. Proceeding 1st Earth Science International Seminar Yogyakarta 29th November, 132–138.

Sarkar, S., & Kanungo, D. P. (2004). *An Integrated Approach for Landslide Susceptibility Mapping Using Remote Sensing and GIS*. 70(5), 617–625.

Soehatman, R. (2010). *Manajemen bencana*. Jakarta: Dian Rakyat.

Souisa M., Hendrajaya L., & Handayani, G. (2015). *Landslide Dynamics and Determination Critical Condition Using of Resistivity Method in Desa Negeri Lima Ambon*. *Indonesian Journal of Physics*, 26 (1), 1–4.

Supriatna S., Sukardi R., Rustandi E. (1995). *Peta Geologi Lembar Samarinda, Kalimantam Timur*, Bandung: Pusat Penelitian dan Pengembangan Geologi

Syaifullah. (2010). *Pengenalan Metode AHP (Analytical Hierarchy Process)*. Wordpress, 1–11.

Taufiq, H.P., dan Suharyadi,(2008) *Landslide Risk Spatial Modelling Using Geographical Information System*. Tutorial Landslide. Laboratorium Sistem Informasi Geografis. Fakultas Geografi Universitas gajah Mada. 9halaman.

Telford, M.W., Geldart, L.P., Sherrif, R.E. and Keys, D.A. 2004. *Applied Geophysics*. Cambridge University Press, Cambridge New York, 556–557.

Tunena, M., & Tamuntuan, G. H. (2018). *Identifikasi Bidang Gelincir Dengan Eksplorasi Geolistrik Dalam Upaya Mitigasi Bencana Alam Tanah Longsor Di Desa Tinoor*. *Jurnal MIPA*, 7(2), 1-5.

Vahidnia, M. H., Alesheikh, A. A., Alimohammadi, A., & Hosseinali, F. (2009). *Landslide Hazard Zonation Using Quantitative Methods in GIS. International Journal of Civil Engineering*, 7(3), 176-189. Diakses dari http://ijce.iust.ac.ir/article-1-289-en.pdf

Wardyaningrum, D. (2014). *Perubahan Komunikasi Masyarakat Dalam Inovasi Mitigasi Bencana di Wilayah Rawan Bencana Gunung Merapi*. *Jurnal ASPIKOM*, 2(3), 179. https://doi.org/10.24329/aspikom.v2i3.69.

Wibowo, A., Widjonarko, D. S., & Wardoyo, A. (2018). *Kajian kerentanan tanah longsor berbasis SIG dan metode AHP di Kabupaten Banjarnegara*. *Jurnal Geografi*, 10(2), 85–94. https://doi.org/10.15294/jg.v10i2.18567.